JOURNAL OF SOLID STATE CHEMISTRY **128,** 273–281 (1997)
ARTICLE NO. SC967218

Temperature-Dependent Structural Properties of the 1,10-Decanedicarboxylic Acid/Urea Inclusion Compound

Lily Yeo,* Kenneth D. M. Harris,* and François Guillaume†

*School of Chemistry, University of Birmingham, Edgbaston, Birmingham B15 2TT, United Kingdom; and
†Laboratoire de Spectroscopie Moléculaire et Cristalline, Université de Bordeaux I, CNRS URA 124, 33405 Talence Cedex, France

Received July 29, 1996; in revised form November 1, 1996; accepted November 7, 1996

Periodic structural properties of the 1,10-decanedicarboxylic acid/urea inclusion compound have been investigated at ambient temperature (high-temperature phase) and at 173 K (low-temperature phase). In the high-temperature phase, the inclusion compound has the hexagonal urea tunnel structure of the conventional urea inclusion compounds, with substantial orientational disorder of the guest molecules. In the low-temperature phase, the urea tunnel structure distorts to form an orthorhombic structure, based on a 2×2×1 supercell of the orthohexagonal cell of the high-temperature structure. There are four independent types of tunnel exhibiting different modes of distortion. Within each type of tunnel there is a comparatively narrow distribution of guest molecule orientations, which correlates well with the observed distortion of the tunnel. The reported results for the 1,10-decanedicarboxylic acid/urea inclusion compound highlight several issues of wider relevance within the context of structural properties of solid inclusion compounds, and these issues are discussed in detail. © 1997 Academic Press

INTRODUCTION

There is currently considerable interest in the structural and dynamic properties of urea inclusion compounds (1, 2). In these solids, the urea molecules form an extensively hydrogen-bonded host structure (3, 4), containing linear, parallel tunnels with guest molecules packed densely along these tunnels. As a consequence of the requirement for size and shape compatibility between the guest molecules and the host tunnels, typical guest molecules for the urea tunnel structure are based on a sufficiently long alkane chain with only a limited degree of substitution permitted.

For most urea inclusion compounds, there is an incommensurate relationship between the periodic repeat distances (denoted c_h and c_g, respectively) of the host and guest substructures along the tunnel axis (classically, for an incommensurate system, sufficiently small integers p and q cannot be found for which $pc_h \approx qc_g$). A more detailed discussion of incommensurate and commensurate behavior in one-dimensional inclusion compounds is given in Ref. (5). Although the host and guest substructures are chemically distinguishable from each other and possess different structural periodicities, these two substructures are not independent, since each substructure exerts an incommensurate modulation upon the other. The host substructure is best considered in terms of a "basic structure" which is subjected to an incommensurate modulation mediated by the guest substructure; the basic structure can be described using conventional crystallographic principles (e.g., three-dimensional space group symmetry). In a similar manner, the guest substructure can be considered in terms of an incommensurately modulated basic structure. The incommensurate modulations describe perturbations to the basic structures which arise as a consequence of host–guest interaction. A full discussion of these structural issues for the urea inclusion compounds is given in Ref. (4).

When this structural description is transformed to reciprocal space, it is clear that an incommensurate urea inclusion compound will give two distinguishable diffraction patterns: the "h" diffraction pattern, which arises from diffraction by the basic host structure (and by the incommensurate modulation within the guest substructure), and the "g" diffraction pattern, which arises from diffraction by the basic guest structure (and by the incommensurate modulation within the host substructure). The reciprocal lattice defining the positions of maxima in the h diffraction pattern is reciprocal to the direct space lattice that defines the periodicity of the basic host structure, and the reciprocal lattice defining the positions of maxima in the g diffraction pattern is reciprocal to the direct space lattice that defines the periodicity of the basic guest structure.

For most conventional urea inclusion compounds, the basic host structure is hexagonal at sufficiently high temperature and the guest molecules are dynamics, and undergo reorientation about the tunnel axis and restricted translation along the tunnel. As the symmetry (hexagonal) of the average basic host structure determined from diffraction is higher than the symmetry of an individual guest molecule, it

0022-4596/97 $25.00

is clear that the observed (average) symmetry of the basic host structure arises from a time-average over the motion of the guest molecules. Most conventional urea inclusion compounds undergo a phase transition (6–8) (or in some cases more than one phase transition) at sufficiently low temperature, and in general these transitions are associated with a lowering of the symmetry of the average host structure (9–12) and a restriction (although not necessarily a cessation) of the motional freedom of the guest molecules (12–17).

Although the dynamic properties of the guest molecules have been probed as a function of temperature for several urea inclusion compounds across the phase transition temperature, less attention has been devoted to changes in the structural properties of the host. In part, this is because multiple crystal twinning usually accompanies the transition from the high-temperature phase (hexagonal) to the low-temperature phase (usually orthorhombic), limiting the prospects for using single crystal X-ray diffraction to investigate structural properties of the low-temperature phase. It has been reported (9, 10) that the hexadecane/urea inclusion compound becomes triply twinned below the transition temperature, with individual twins related by 120° rotation about the tunnel axis. In view of this twinning, powder diffraction represents, in principle, a more straightforward approach for structure determination of the low-temperature phase, and this technique has been used to establish structural aspects of the low-temperature phases of the hexadecane/urea (11) and 1,10-dibromodecane/urea (12) inclusion compounds.

In this paper, we report structural properties of the 1,10-decanedicarboxylic acid/urea inclusion compound as a function of temperature. In the low-temperature phase (at 173 K) there is no evidence of crystal twinning allowing structural properties to be determined from single crystal X-ray diffraction data (h diffraction pattern). This structure exhibits several interesting features, particularly concerning the orientational ordering of the guest molecules and its relation with the distortion in the host tunnel structure. Structural properties at ambient temperature are also reported.

EXPERIMENTAL

The 1,10-decanedicarboxylic acid/urea inclusion compound was prepared from commercially available reagents using the following method. An excess amount of 1,10-decanedicarboxylic acid (excess with respect to the expected guest/host molar ratio in the inclusion compound) was added to a saturated solution of urea in methanol in a conical flask under ultrasonic agitation at ca. 55°C. Extra methanol was added to dissolve crystals of inclusion compound which precipitated immediately upon mixing. The flask was then transferred to an incubator, in which it was cooled from 55 to 15°C over a period of 24 h. When sufficiently large crystals had grown (generally after a few days) they were collected and washed with 2,2,4-trimethylpentane. The crystals had a hexagonal prismatic morphology and their behavior in the polarizing microscope was consistent with their assignment to the hexagonal crystal system. Powder X-ray diffraction indicated that the sample prepared did not contain any significant amount of the "pure" crystalline phase of urea (the crystal structure of which differs substantially from the urea substructure in urea inclusion compounds).

To confirm the occurrence of a low-temperature phase transition in the 1,10-decanedicarboxylic acid/urea inclusion compound, differential scanning calorigrams were recorded (18) with the sample subjected to a cycle of cooling and heating between 298 and 98 K at a rate of 10 K min^{-1}. On cooling, an exotherm is obseved at 203 K (enthalpy change -0.46 J g^{-1}), whereas on warming, an endotherm is observed at 204 K (peak maximum temperature; enthalpy change 0.55 J g^{-1}). (Note that the quoted temperatures correspond to the peak maxima.) This result identifies two temperature regimes for 1,10-decanedicarboxylic acid/urea, denoted the high-temperature phase (above ca. 203 K) and the low-temperature phase (below ca. 203 K).

All single-crystal X-ray diffraction experiments were carried out using graphite-monochromated Mo$K\alpha$ radiation ($\lambda = 0.71073$ Å) on a Rigaku R-Axis II diffractometer equipped with an area detector. A standard MSC low-temperature device was used for experiments below ambient temperature (the stability and accuracy of the low-temperature device have been determined to be ca. $\pm$ 2 K). Single-crystal X-ray diffraction rotation photographs were recorded, as a function of temperature, with the rotation axis parallel to the main axis of the hexagonal prismatic morphology of the crystals (tunnel axis of the urea host structure). The same crystal was used for the experiments at ambient temperature and low temperature, with the experiments at ambient temperature performed first. For the low temperature experiments, the crystal was allowed about 2 h to reach thermal equilibrium before starting the X-ray diffraction measurements. Both data collections comprised 72 frames, each recorded over an oscillation range of 5° with 10 min exposure time per frame. The crystal to detector distance was 100 mm in both cases. No corrections were made for X-ray absorption.

DATA ANALYSIS

The reported data collections at ambient temperature and 173 K constitute measurements of the h diffraction data. As discussed in Ref. (2), structure determination calculations using the h diffraction data allow the basic host structure to be determined, as well as providing some information concerning the guest substructure. First, the ($hk0$) reflections (which are common to both the h and g

diffraction patterns) provide two-dimensional information on the basic guest structure projected onto the plane perpendicular to the tunnel axis. Second, the h reflections $(hkl)_h$ with $l \neq 0$ convey information on the incommensurate perturbations to the basic guest structure (these perturbations, which arise from host–guest interaction, have the same periodicity as the basic host structure). This "perturbation electron density" represents the difference in electron density between the true guest substructure averaged over the periodicity of the basic host structure and the basic guest structure averaged over the periodicity of the basic host structure. Although this "perturbation electron density" conveys important structural information, it is more satisfactory to seek a comprehensive understanding of the incommensurate modulations in incommensurate inclusion compounds by structure determination of the composite inclusion compound in a four-dimensional superspace group (19–21) (considering both h and g diffraction data together). Unfortunately, such analysis is not feasible in the present case as there are only very few Bragg diffraction maxima of significant intensity in the g diffraction pattern. Thus, in summary, structure determination calculations using the h diffraction data yield: (a) the average basic host structure; and (b) an average guest electron distribution, which has a straightforward physical interpretation when projected onto the plane perpendicular to the tunnel axis.

In structure refinement, the method of introducing the contributions from the guest electron density requires special attention, and the following strategy was followed. For the nonhydrogen atoms of urea, positional parameters (taken initially from the results of the structure solution calculation) and anisotropic atomic displacement parameters were refined in the conventional manner. The difference Fourier map for this host-only structural model contained significant maxima located within the tunnel, clearly representing guest electron density. A carbon atom was added in the position of the highest maximum in the difference Fourier map, and its positional parameters and isotropic atomic displacement parameter were refined along with the parameters for the nonhydrogen atoms of the host structure (as expected, the refined values of the isotropic atomic displacement parameters for the carbon atoms in the tunnel are significantly higher than the equivalent isotropic atomic displacement parameters for the atoms of the urea molecules). This procedure was repeated, adding one carbon atom at a time, until the highest peak in the difference Fourier map represented the position of a urea hydrogen atom. Finally, hydrogen atoms were added to the urea molecules according to standard geometric features and refined using a "riding" model (i.e., the coordinate shifts for the hydrogen atom and the nitrogen atom to which it is attached are the same). The isotropic atomic displacement parameter of each hydrogen atom was refined as 1.2 times the equivalent isotropic atomic displacement parameter of the nitrogen atom to which it is attached.

Structure solution calculations were carried out using the direct methods program SIR-92, and structure refinement calculations were carried out using the SHELXL-93 program. The following agreement factors have been used (see Tables 1 and 2):

$$R = \frac{\sum \| F_o| - |F_c \|}{\sum |F_o|}$$

$$R_w = \left(\frac{\sum w [F_o^2 - F_c^2]^2}{\sum w [F_o^2]^2} \right)^{1/2}.$$

RESULTS AND DISCUSSION

At ambient temperature, powder X-ray diffraction indicates that the 1,10-decanedicarboxylic acid/urea inclusion compound has the hexagonal basic host structure of the conventional urea inclusion compounds. The single-crystal X-ray diffraction rotation photograph is shown in Fig. 1, the structure determined from the measured h diffraction data is viewed along the tunnel axis in Fig. 2, and structural parameters are given in Table 1. From the rotation photograph, the characteristics of the basic guest structure are qualitatively similar to those established previously (22) for α,ω-dibromoalkane/urea inclusion compounds, for which $\Delta_g = c_g/3$ (Δ_g represents the offset along the tunnel axis between the centres of mass of guest molecules in adjacent tunnels (23)). A detailed characterization of the basic guest structure in the 1,10-decanedicarboxylic acid/urea inclusion compound will form the basis of a future investigation. The diffuse scattering (in high index layers) in the g diffraction pattern suggests that there is some loss of three-dimensional ordering of the guest molecules in directions perpendicular to the tunnel axis.

We now consider the structural properties of the low-temperature phase. The single-crystal X-ray diffraction rotation photograph recorded at 173 K is shown in Fig. 3. There is no evidence for the generation of any superstructure along the tunnel direction (i.e., no new layer lines appear in the h diffraction pattern). However, the h diffraction pattern is different from that at ambient temperature, particularly in terms of the number and arrangement of discrete diffraction maxima within the layer lines. These facts are accounted for completely by the structural properties discussed below. The structure determined from the measured h diffraction data is viewed along the tunnel axis in Fig. 4, and structural parameters are given in Table 2.

The basic host structure in the low-temperature phase has orthorhombic metric symmetry, and the unit cell is a $2 \times 2 \times 1$ supercell of the orthohexagonal description of the basic host structure in the high-temperature phase. Viewed along the tunnel axis (Fig. 4), the distortion of the tunnels

TABLE 1
Structural Parameters Determined from the "h" Diffraction Pattern for the 1,10-Decanedicarboxylic Acid/Urea Inclusion Compound at Ambient Temperature and Other Information Relating to the Structure Refinement Calculation

Atom	$x/\lvert a_h\rvert$	$y/\lvert b_h\rvert$	$z/\lvert c_h\rvert$	$U_{11}/\text{Å}^2$	$U_{22}/\text{Å}^2$	$U_{33}/\text{Å}^2$	$U_{23}/\text{Å}^2$	$U_{13}/\text{Å}^2$	$U_{12}/\text{Å}^2$	$U_{iso}/\text{Å}^2$
O1	0.6408(3)	0.3204(2)	0.58333(0)	0.040(2)	0.051(1)	0.033(2)	− 0.0001(8)	0.0000(0)	0.0202(8)	
N1	0.9119(3)	0.4342(4)	0.6858(2)	0.043(1)	0.081(2)	0.036(2)	0.001(1)	− 0.0032(8)	0.024(1)	
C1	0.8168(5)	0.4084(2)	0.58333(0)	0.045(2)	0.042(2)	0.031(2)	− 0.003(1)	0.0000(0)	0.022(1)	
C2	− 0.045(4)	0.0000(0)	0.0000(0)							0.38(2)
C3	0.075(4)	0.0000(0)	0.0000(0)							0.37(2)

Note. C2 and C3 denote carbon atoms added within the tunnel to represent the contribution to the "h" diffraction pattern from scattering by the guest molecules. The asymmetric unit of the host structure comprises one half urea molecule, with its C=O bond lying on a two-fold axis (special position $(2\bar{x}, \bar{x}, 7/12)$). There are six urea molecules in the unit cell.

Space group	$P6_122$
Lattice parameters	$\lvert a_h\rvert = 8.237(2)$ Å
	$\lvert c_h\rvert = 11.001(2)$ Å
Number of unique reflections with $\lvert F_0\rvert > 4\sigma(F_0)$	264
R	0.0455
R_w	0.1653
Weight	$1/[\sigma(F_0)^2 + (0.1623^* P)^2 + 0.07P]$, where $P = [\max(F_0^2, 0) + 2F_c^2]/3$
Number of parameters refined	24
Bond lengths/Å	
O1–C1	1.255(4)
N1–C1	1.328(3)
Bond angle/°	
O1–C1–N1	120.7(2)

TABLE 2
Structural Parameters Determined from the "h" Diffraction Pattern for the 1,10-Decanedicarboxylic Acid/Urea Inclusion Compound at 173 K and Other Information Relating to the Structure Refinement Calculation

Atom	$x/\lvert a_h\rvert$	$y/\lvert b_h\rvert$	$z/\lvert c_h\rvert$	$U_{11}/\text{Å}^2$	$U_{22}/\text{Å}^2$	$U_{33}/\text{Å}^2$	$U_{23}/\text{Å}^2$	$U_{13}/\text{Å}^2$	$U_{12}/\text{Å}^2$
O1	− 0.2419(3)	0.4195(1)	0.5837(4)	0.027(3)	0.045(2)	0.031(3)	0.0001(3)	− 0.020(2)	− 0.001(2)
O2	− 0.2645(3)	0.4193(1)	− 0.0833(4)	0.018(3)	0.054(3)	0.033(3)	− 0.007(3)	− 0.012(2)	− 0.006(2)
O3	0.0000(0)	0.3433(2)	− 0.2500(0)	0.044(5)	0.049(4)	0.032(4)	0.000(0)	− 0.014(3)	0.000(0)
O4	0.0000(0)	0.1640(2)	0.2500(0)	0.029(4)	0.029(3)	0.038(3)	0.000(0)	0.008(3)	0.000(0)
O5	− 0.2543(2)	0.4078(1)	0.2510(3)	0.049(4)	0.031(2)	0.034(3)	− 0.002(2)	− 0.015(2)	− 0.001(2)
O6	0.0111(3)	0.1750(1)	0.5832(4)	0.055(3)	0.028(2)	0.034(3)	− 0.001(2)	0.021(3)	0.010(2)
O7	− 0.0116(3)	0.3328(1)	0.0833(4)	0.063(4)	0.036(2)	0.028(3)	0.003(2)	− 0.013(3)	− 0.008(2)
N1	− 0.2705(4)	0.4782(2)	0.1482(5)	0.072(5)	0.043(3)	0.027(3)	− 0.001(3)	− 0.009(3)	− 0.008(3)
N2	0.0094(4)	0.2319(2)	0.3520(5)	0.057(4)	0.035(3)	0.031(3)	− 0.0023(2)	− 0.001(3)	− 0.005(3)
N3	0.0091(5)	0.2755(2)	− 0.3529(4)	0.087(5)	0.034(3)	0.023(3)	− 0.009(2)	− 0.005(3)	0.016(3)
N4	− 0.0864(4)	0.1347(2)	0.4796(5)	0.039(4)	0.054(3)	0.031(3)	− 0.007(2)	0.019(3)	− 0.010(3)
N5	− 0.2448(4)	0.4779(2)	0.3531(5)	0.089(5)	0.039(3)	0.022(3)	− 0.001(3)	− 0.005(3)	0.010(3)
N6	− 0.3375(4)	0.3777(2)	0.4797(5)	0.049(4)	0.064(4)	0.032(3)	− 0.004(3)	− 0.015(3)	− 0.016(3)
N7	0.0993(4)	0.3611(2)	0.1861(5)	0.053(4)	0.066(4)	0.031(3)	0.005(3)	− 0.022(3)	− 0.027(3)
N8	− 0.1552(4)	0.3935(2)	− 0.1860(5)	0.037(4)	0.063(4)	0.030(3)	− 0.005(3)	− 0.011(3)	0.008(3)
N9	− 0.1002(4)	0.1466(2)	0.6867(5)	0.049(4)	0.057(4)	0.037(3)	− 0.011(3)	0.016(3)	− 0.019(3)
N10	− 0.3504(4)	0.3895(2)	0.6868(5)	0.050(4)	0.056(4)	0.029(3)	− 0.003(3)	− 0.007(3)	− 0.005(3)
N11	− 0.1662(4)	0.3811(2)	0.0205(5)	0.058(5)	0.067(4)	0.029(3)	− 0.005(3)	− 0.022(3)	0.022(3)
N12	0.0860(4)	0.3729(2)	− 0.0210(5)	0.049(4)	0.058(4)	0.034(3)	0.009(3)	− 0.022(3)	− 0.015(3)
C1	0.0530(4)	0.3558(2)	0.0817(6)	0.027(4)	0.029(3)	0.032(4)	− 0.001(3)	− 0.020(3)	0.004(3)
C2	− 0.0539(4)	0.1523(2)	0.5825(6)	0.022(4)	0.025(3)	0.041(4)	0.005(3)	0.020(3)	0.009(2)
C3	− 0.3088(4)	0.3967(2)	0.5844(6)	0.054(5)	0.051(4)	0.028(4)	− 0.003(4)	− 0.020(4)	− 0.003(3)
C4	0.0000(0)	0.2995(3)	− 0.2500(0)	0.037(6)	0.027(5)	0.040(6)	0.000(0)	− 0.009(5)	0.000(0)
C5	− 0.1954(5)	0.3991(2)	− 0.0832(6)	0.055(6)	0.052(4)	0.034(4)	− 0.007(4)	− 0.028(4)	− 0.004(4)
C6	− 0.2559(4)	0.4536(2)	0.2510(5)	0.038(5)	0.051(4)	0.030(4)	0.003(4)	− 0.006(3)	− 0.003(3)
C7	0.0000(0)	0.2077(3)	0.2500(0)	0.023(6)	0.031(4)	0.033(5)	0.000(0)	0.019(4)	0.000(0)

Table 2 – *Continued*

Atom	$x/\lvert a_h\rvert$	$y/\lvert b_h\rvert$	$z/\lvert c_h\rvert$	$U_{iso}/\text{Å}^2$
C8	0.455(2)	0.000(0)	0.000(0)	0.21(1)
C9	0.485(3)	0.491(4)	− 0.02(1)	0.48(4)
C10	0.758(2)	0.268(1)	− 0.161(3)	0.25(1)
C11	0.733(2)	0.2298(8)	0.190(2)	0.206(9)
C12	0.968(2)	0.4916(9)	0.133(2)	0.24(1)
C13	0.703(3)	0.235(1)	− 0.015(4)	0.34(2)
C14	0.490(1)	0.4659(9)	0.130(2)	0.215(9)
C15	0.724(2)	0.242(1)	− 0.531(3)	0.26(1)
C16	0.555(3)	0.000(0)	0.000(0)	0.37(3)
C17	0.727(2)	0.235(2)	− 0.236(5)	0.36(2)
C18	0.000(0)	− 0.019(3)	0.250(0)	0.37(3)
C19	0.738(2)	0.2556(8)	− 0.405(3)	0.207(8)
C20	0.501(3)	0.476(1)	− 0.162(3)	0.37(2)
C21	0.545(2)	− 0.001(1)	0.228(4)	0.33(2)

Note. C8 to C21 denote carbon atoms added within the tunnel to represent the contribution to the h diffraction pattern from scattering by the guest molecules. The asymmetric unit of the host structure comprises (a) five urea molecules in general positions; and (b) two half urea molecules with their C=O bonds lying on two-fold axes (atoms C4 and O3 on special positions (0, $\bar{y}$, 3/4) and atoms C7 and O4 on special positions (0, y, 1/4)). There are 48 urea molecules in the unit cell.

Space group	$C222_1$
Lattice parameters	$\lvert a_h\rvert = 16.305(5)$ Å $\lvert b_h\rvert = 28.321(8)$ Å $\lvert c_h\rvert = 11.000(2)$ Å
Number of unique reflections with $\lvert F_o\rvert > 4\sigma(F_o)$	2637
R	0.1074
R_w	0.3408
Weight	$1/[\sigma(F_o)^2 + (0.1623^* P)^2 + 15.65P]$, where $P = [\max(F_o^2, 0) + 2F_c^2]/3$
Number of parameters refined	269

Bond lengths/Å

O1–C3	1.267(8)	N1–C6	1.349(8)
O2–C5	1.264(8)	N2–C7	1.323(6)
O3–C4	1.24(1)	N3–C4	1.328(6)
O4–C7	1.240(9)	N4–C2	1.347(8)
O5–C6	1.299(8)	N5–C6	1.328(8)
O6–C2	1.239(7)	N6–C3	1.355(8)
O7–C1	1.240(7)	N7–C1	1.383(7)
		N8–C5	1.316(7)
		N9–C2	1.382(8)
		N10–C3	1.331(7)
		N11–C5	1.338(8)
		N12–C1	1.336(8)

Bond angles/°

O7–C1–N7	120.5(6)	O3–C4–N3	120.8(4)
O7–C1–N12	123.2(5)	O2–C5–N8	119.8(6)
N7–C1–N12	116.1(6)	O2–C5–N11	119.4(6)
O6–C2–N4	122.3(5)	N8–C5–N11	120.6(7)
O6–C2–N9	121.6(6)	O5–C6–N1	121.2(5)
N4–C2–N9	115.9(5)	O5–C6–N5	121.0(5)
O1–C3–N6	119.6(6)	N1–C6–N5	117.8(6)
O1–C3–N10	121.5(6)	O4–C7–N2	121.1(4)
N6–C3–N10	118.8(6)		

from the hexagonal high-temperature structure is clearly evident. There are eight tunnels per unit cell (*ab* plane), but because of the C-centering there are only four independent tunnels. The degree of distortion of these tunnels is best indicated (Fig. 5) by considering the "diameters" between opposite corners of the (irregular) hexagonal projections of each tunnel. For three of the four independent types of tunnel (type A), one diameter is significantly longer than the other two, whereas for the other type of tunnel (type B), two diameters are significantly longer than the other one.

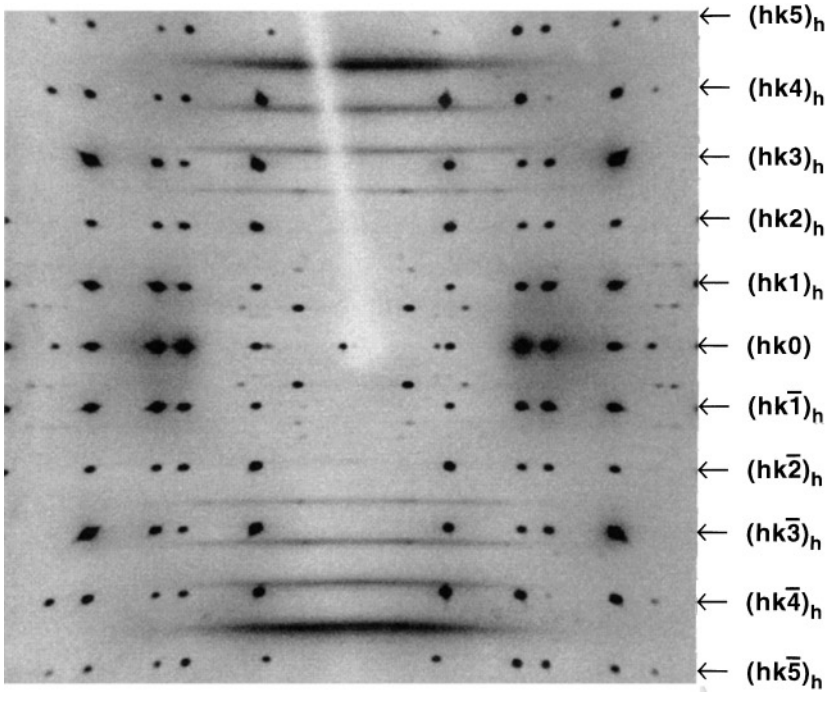

FIG. 1. Single-crystal X-ray diffraction rotation photograph, recorded at ambient temperature, for the 1,10-decanedicarboxylic acid/urea inclusion compound rotating about the tunnel axis. Layer lines of the h diffraction pattern are indexed (the X-ray scattering between these layer lines represents the g diffraction pattern).

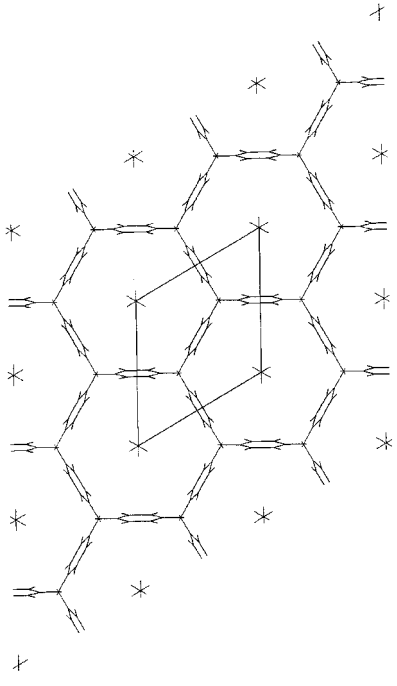

FIG. 2. Structure of the 1,10-decanedicarboxylic acid/urea inclusion compound, determined at ambient temperature, viewed along the tunnel axis (crystallographic *c* axis). The atoms within the tunnel have been added to represent the contribution to the h diffraction pattern from scattering by the guest molecules—the physical significance of these atom positions is discussed in the text.

Intuitively, this would suggest that if the guest molecules become orientationally ordered in the low-temperature phase, the preferred direction (in projection) of the plane of the guest molecule should be different for the tunnels of type A (plane of guest molecule oriented along the long diameter) than for the tunnels of type B (plane of guest molecule oriented perpendicular to the short diameter). These expectations are indeed borne out in practice, as evident (see Fig. 4) from the observed projection of the guest electron density onto the plane perpendicular to the tunnel axis. It is clear from these results that the geometric distortions of the host tunnel are related to orientational ordering of the guest molecules. The dynamic properties of the guest molecules in the 1,10-decanedicarboxylic acid/urea inclusion compound have not yet been studied, but it is clear that there is a substantial increase in the orientational ordering of the guest molecules in the low-temperature phase.

Although the structural properties of the guest molecules will be the basis of a detailed future investigation, some preliminary comments of a qualitative nature can be made on the basis of changes observed in the g diffraction pattern (compare Figs. 1 and 3). First, an increase in the extent of three-dimensional ordering of the guest molecules is evident from the increased localization of intensity at specific positions within the diffuse bands in the g diffraction pattern. However, the fact that some diffuse character remains in these layer lines alludes to the continued existence of some disorder within the basic guest structure, but nevertheless

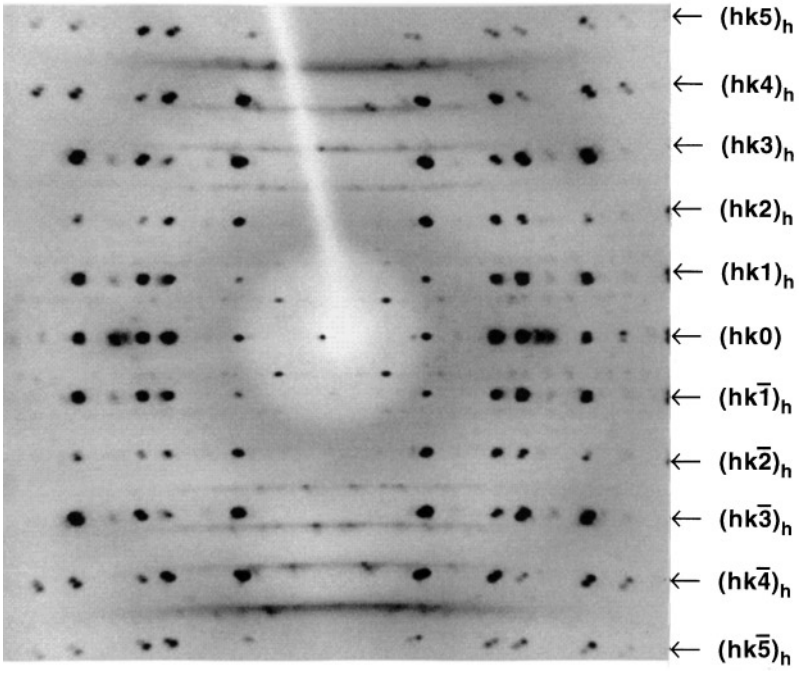

FIG. 3. Single-crystal X-ray diffraction rotation photograph, recorded at 173 K, for the 1,10-decanedicarboxylic acid/urea inclusion compound rotating about an axis close to the tunnel axis. Layer lines of the h diffraction pattern are indexed (the X-ray scattering between these layer lines represents the g diffraction pattern).

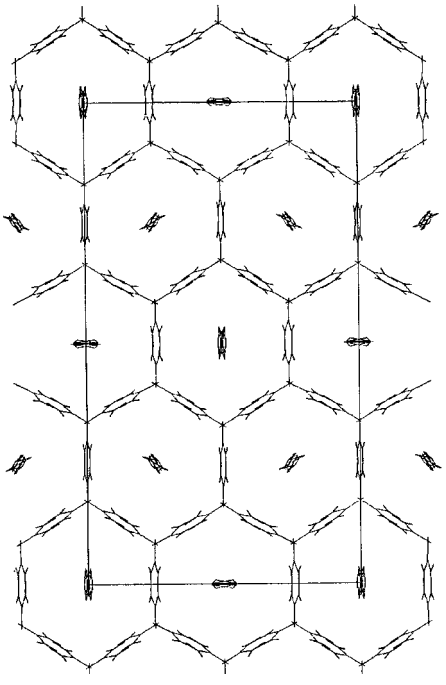

FIG. 4. Structure of the 1,10-decanedicarboxylic acid/urea inclusion compound, determined at 173 K, viewed along the tunnel axis (crystallographic *c* axis). The atoms within the tunnel have been added to represent the contribution to the h diffraction pattern from scattering by the guest molecules—the physical significance of these atom positions is discussed in the text.

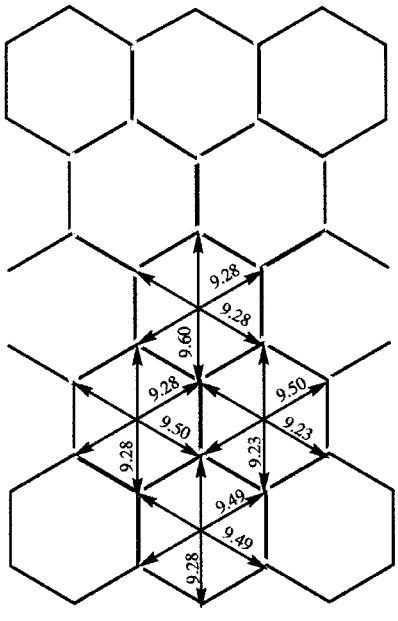

FIG. 5. Geometrical characteristics of the "distorted" host tunnel structure in the 1,10-decanedicarboxylic acid/urea inclusion compound at 173 K. Distances are given in Å units.

the extent of three-dimensional ordering is substantially greater than at ambient temperature. Clearly the orientational ordering of guest molecules evident from Fig. 4 cannot be consistent with the lattice with rhombohedral metric symmetry that corresponds to the $\Delta_g = c_g/3$ condition observed at ambient temperature, and the symmetry of the (average) basic guest structure is lowered on entering the low-temperature phase (rhombohedral in the high-temperature phase, *probably* becoming orthorhombic in the low-temperature phase). The relative positions of the layer lines for the h and g diffraction patterns in Fig. 3 implies that there is an incommensurate relationship between the host and guest substructures along the tunnel axis in the low-temperature phase.

CONCLUDING REMARKS

The structure of the low-temperature phase of the 1,10-decanedicarboxylic acid/urea inclusion compound represents, to our knowledge, the first satisfactory structure determination for the low-temperature phase of a urea inclusion compound for which the high-temperature phase has the conventional urea tunnel structure. It is clear that, within each tunnel, there is a comparatively narrow distribution of guest molecule orientations, which correlates well with the observed distortions of the host tunnel. While the guest molecules become orientationally ordered with respect to the host structure on entering the low-temperature phase, there is still an incommensurate relationship between the periodicities of the host and guest substructures along the tunnel, with no evidence for the two substructures locking into a commensurate phase at low temperature. Several issues devolve upon the observations made here and have wider relevance within the context of structural properties of solid inclusion compounds.

Before raising some of these issues, we recall that the following are important in determining the observed (optimum) structure of a urea inclusion compound: host–host interaction, host–guest interaction, intratunnel guest–guest interaction, and intertunnel guest–guest interaction. Intramolecular potential energies of the host and guest molecules are neglected from this discussion, as the urea molecules exist in a well-defined conformational state and the 1,10-decanedicarboxylic acid molecules cannot have significant latitude for conformational flexibility when constrained within the urea tunnel structure.

First, we consider ordering of the guest molecules within a given tunnel. Clearly the distortion of the urea tunnel structure on entering the low-temperature phase is related to optimization of the host–host and/or host–guest interactions, and the concomitant orientational ordering of the guest molecules is related to optimization of the host–guest interactions. In general, the guest molecule orientation (with respect to reorientation about the tunnel axis) corresponding to minimum host–guest interaction energy for an individual guest molecule should be expected to vary as a function of the z coordinate of the guest molecule relative to the unit cell of the basic host structure (as demonstrated previously (24) for the conventional urea tunnel structure (hexagonal high-temperature phase)). For an incommensurate urea inclusion compound, each guest molecule within a given tunnel occupies, in principle, a different position (z coordinate) relative to the unit cell of the basic host structure, and each guest molecule might therefore be expected to have a different orientation. As a narrow distribution of guest molecule orientations is implicated for the low-temperature phase of 1,10-decanedicarboxylic acid/urea, then presumably (i) the preferred guest molecule orientation due to host–guest interaction must be essentially the same for all positions of the guest molecule along the tunnel (e.g., as a result of the distortion of the host tunnel); and/or (ii) other factors, in addition to host–guest interaction, are important in determining the relative orientations of the guest molecules. The intratunnel guest–guest interaction may be particularly important in this regard. For 1,10-decanedicarboxylic acid/urea, the intratunnel guest–guest interaction is probably the characteristic double hydrogen bonded arrangement between two carboxylic acid groups, and this interaction should strongly promote a situation in which all guest molecules within a given tunnel have the same orientation.

Next, we consider the orientational ordering of the guest molecules in different tunnels, recalling that a large unit cell ($2 \times 2 \times 1$ supercell of the orthohexagonal description of the high-temperature phase) is required to describe the distortion of the basic host structure and the concomitant orientational ordering of the guest molecules. Distortion of the basic host structure and orientational ordering of the guest molecules could, in principle, be achieved within much smaller unit cells, as discussed previously (7, 9, 10) for alkane/urea inclusion compounds. Evidently, the situation for 1,10-decanedicarboxylic acid/urea is more complex than that for the alkane/urea inclusion compounds, and it is unlikely that the structural properties of the low-temperature phase of 1,10-decanedicarboxylic acid/urea can be rationalized using models of the type discussed previously (10). The fact that different tunnels in 1,10-decanedicarboxylic acid/urea distort selectively in different ways (giving rise to the $2 \times 2 \times 1$ supercell) implies that optimization of host–host interactions and host–guest interactions cannot be the only factors dictating the structural distortions of the tunnels and the orientational ordering of the guest molecules (if they were the only factors, we should expect that all tunnels would distort in the same manner). It is plausible that intertunnel guest–guest interactions may influence significantly the specific mode of orientational ordering of the guest molecules, promoting the $2 \times 2 \times 1$ supercell rather than simpler alternative orientationally ordered structures.

In this regard, the carboxylic acid groups of the guest molecules may be important in promoting the observed mode of orientational ordering. A detailed understanding of the factors governing the orientational ordering of the guest molecules should become clearer when a greater amount of structural information is available on the low-temperature phases of urea inclusion compounds containing other families of guest molecules with different functional groups.

ACKNOWLEDGMENTS

We are grateful to the following for financial support: Ciba Geigy plc (studentship to L.Y.), the Nuffield Foundation (Science Research Fellowship to K.D.M.H.) and N.A.T.O., the British Council and the French Government (travel grants to F.G. and K.D.M.H.). We thank Dr. E. H. Bocanegra (Universidad del Pais Vasco, Spain) for recording the differential scanning calorimetry data discussed in the text.

REFERENCES

1. K. Takemoto and N. Sonoda, *in* "*Inclusion Compounds*" (J. L. Atwood, J. E. D. Davies, and D. D. MacNicol, Eds.), Vol. **2,** p. 47. Academic Press, New York, 1984.
2. M. D. Hollingsworth and K. D. M. Harris, *in* "*Comprehensive Supramolecular Chemistry*" (D. D. MacNicol, F. Toda, and R. Bishop, Eds.), Vol. **6,** p. 177. Pergamon Press, Elmsford, NY, 1996.
3. A. E. Smith, *Acta Crystallogr.* **5,** 224 (1952).
4. K. D. M. Harris and J. M. Thomas, *J. Chem. Soc. Faraday Trans.* **86,** 2985 (1990).
5. A. J. O. Rennie and K. D. M. Harris, *Proc. R. Soc. A* **430,** 615 (1990).
6. N. G. Parsonage and L. A. K. Staveley, "*Disorder in Crystals*," Oxford Univ. Press, Oxford, 1978.
7. R. M. Lynden-Bell, *Mol. Phys.* **79,** 313 (1993).
8. K. D. M. Harris, *J. Solid State Chem.* **106,** 83 (1993).
9. Y. Chatani, Y. Taki, and H. Tadokoro, *Acta Crystallogr. B* **33,** 309 (1977).
10. Y. Chatani, H. Anraku, and Y. Taki, *Mol. Cryst. Liq. Cryst.* **48,** 219 (1978).
11. K. D. M. Harris, I. Gameson, and J. M. Thomas, *J. Chem. Soc. Faraday Trans.* **86,** 3135 (1990).
12. A. E. Aliev, S. P. Smart, I. J. Shannon, and K. D. M. Harris, *J. Chem. Soc. Faraday Trans.* **92,** 2179 (1996).
13. H. L. Casal, D. G. Cameron, and E. C. Kelusky, *J. Chem. Phys.* **80,** 1407 (1984).
14. K. D. M. Harris and P. Jonsen, *Chem. Phys. Lett.* **154,** 593 (1989).
15. A. El Baghdadi, E. J. Dufourc, and F. Guillaume, *J. Phys. Chem.* **100,** 1746 (1996).
16. F. Guillaume, C. Sourisseau, and A.-J. Dianoux, *J. Chim. Phys. (Paris)* **88,** 1721 (1991).
17. S. P. Smart, F. Guillaume, K. D. M. Harris, and A.-J. Dianoux, *J. Phys. Condens. Matter* **6,** 2169 (1994).
18. L. Yeo, E. H. Bocanegra, K. D. M. Harris, and F. Guillaume, in preparation.
19. S. van Smaalen, *Crystallogr. Rev.* **4,** 79 (1995).
20. S. van Smaalen and K. D. M. Harris, *Proc. R. Soc. A* **452,** 677 (1996).
21. R. Lefort, J. Etrillard, B. Toudic, F. Guillaume, T. Breczewski, and P. Bourges, *Phys. Rev. Lett.* **77,** 4027 (1996).
22. K. D. M. Harris, S. P. Smart, and M. D. Hollingsworth, *J. Chem. Soc. Faraday Trans.* **87,** 3423 (1991).
23. K. D. M. Harris and M. D. Hollingsworth, *Proc. R. Soc. A* **431,** 245 (1990).
24. A. R. George and K. D. M. Harris, *J. Mol. Graphics* **13,** 138 (1995).